Supplementary Information

for

Significant geometry and charge difference between the E_5^{4-} bare clusters of Group 14 Zintl anions and their coordinated form in $[E_5\{M(CO)_3\}_2]^{4-}$ (E=Si, Ge, Sn, Pb; M=Cr, Mo, W) complexes

Yasin Gholiee[*,†], *Sadegh Salehzadeh*[*,‡] *and Shiva Khodaveisi*[‡]

† Department of Chemistry, Faculty of Science, Malayer University, Malayer, Iran

‡ Faculty of Chemistry, Bu-Ali Sina University, Hamedan, Iran

List of Contents:

Table S1. Electronic energies (Hartree) for optimized structures for E_5^n $(E = Si, Ge, Sn, Pb; n = -4, -2, 0)$ clusters from different initial structures, at BP86/def2-TZVPP level of theory.

Table S2. Electronic energies (Hartree) for optimized structures for E_5^n $(E = Si, Ge, Sn, Pb; n = -4, -2, 0)$ clusters from different initial structures, at M06-2X/def2-TZVPP level of theory.

Table S3. The computed and experimental E−E distances (Å) and E−E−E angles (°) for trigonal bipyramid E_5^{2-} $(E = Si, Ge, Sn, Pb)$ clusters, at M06-2X/def2-TZVPP level of theory.

Table S4. The computed and experimental E−E distances (Å) and E−E−E angles (°) for trigonal bipyramid E_5^{2-} $(E = Si, Ge, Sn, Pb)$ clusters, at BP86/def2-TZVPP level of theory.

Table S5. Computed and experimental structural parameters for $[Pb_5\{Mo(CO)_3\}_2]^{4-}$.

Table S6. Computed bond lengths (Å) for $[E_5\{Cr(CO)_3\}_2]^{4-}$ complexes (E=Si, Ge, Sn and Pb), at M06-2X/def2-TZVPP level of theory.

Table S7. Computed bond lengths (Å) for $[E_5\{Mo(CO)_3\}_2]^{4-}$ complexes (E=Si, Ge, Sn and Pb), at M06-2X/def2-TZVPP level of theory.

Table S8. Computed bond lengths (Å) for $[E_5\{W(CO)_3\}_2]^{4-}$ complexes (E=Si, Ge, Sn and Pb), at M06-2X/def2-TZVPP level of theory.

Table S9. Calculated values of uncorrected interaction energies between the fragments (IE, kcal/mol), for $[E_5\{M(CO)_3\}_2]^{4-}$; (E = Si, Ge, Sn and Pb; M = Cr, Mo and W) complexes, at M06-2X/def2-TZVPP level of theory.

Table S10. Calculated values of uncorrected interaction energies between the fragments (IE, kcal/mol), for $[E_5\{M(CO)_3\}_2]^{4-}$; (E = Si, Ge, Sn and Pb; M = Cr, Mo and W) complexes, at BP86/def2-TZVPP level of theory.

Table S11. Calculated values of corrected interaction energies between the fragments (IE, kcal/mol), for $[E_5\{M(CO)_3\}_2]^{4-}$; (E = Si, Ge, Sn and Pb; M = Cr, Mo and W) complexes, at BP86/def2-TZVPP level of theory.

Table S12. Wiberg bond indices (WBIs) for $[E_5\{Cr(CO)_3\}_2]^{4-}$ at M06-2X/def2-TZVPP level of theory.

Table S13. Wiberg bond indices (WBIs) for $[E_5\{Mo(CO)_3\}_2]^{4-}$ at M06-2X/def2-TZVPP level of theory.

Table S14. Wiberg bond indices (WBIs) for $[E_5\{W(CO)_3\}_2]^{4-}$ at M06-2X/def2-TZVPP level of theory.

Table S15. Calculated frequencies (cm^{-1}) for CO stretching bands in $[E_5\{Cr(CO)_3\}_2]^{4-}$ complexes as well as bond lengths (Å) and Wiberg bond indices (WBIs) for M-C and C-O bonds.

Table S16. Calculated frequencies (cm^{-1}) for CO stretching bands in $[E_5\{Mo(CO)_3\}_2]^{4-}$ complexes as well as bond lengths (Å) and Wiberg bond indices (WBIs) for M-C and C-O bonds.

Table S17. Calculated frequencies (cm^{-1}) for CO stretching bands in $[E_5\{W(CO)_3\}_2]^{4-}$ complexes as well as bond lengths (Å) and Wiberg bond indices (WBIs) for M-C and C-O bonds.

Table S18. Energy decomposition analysis results between $[E_5\{M(CO)_3\}]^{4-}$ and {M(CO)$_3$} fragments (A−BA') in $[E_5\{M(CO)_3\}_2]^{4-}$ $complexes$ (E=Si, Ge, Sn and Pb; M=Cr, Mo and W) at BP86-D3/TZP(ZORA) level of theory.

Table S19. Comparison of computed Ge−Ge distances (Å) for trigonal bipyramid Ge_5^{2-} cluster in Ref. 43 and in this study.

Table S20. Comparison of computed Ge−Ge distances (Å) for trigonal bipyramid Ge_5 cluster in Ref. 43 and in this study.

Figure S1. Optimized structures of $E_5^n\ (E = Si, Ge, Sn, Pb; n = -4, -2, 0)$ clusters from square pyramid initial (C_{4v}) geometry, at M06-2X/def2-TZVPP level of theory.

Figure S2. Optimized structures of $E_5^n\ (E = Si, Ge, Sn, Pb; n = -4, -2, 0)$ clusters from trigonal bipyramid (D_{3h}) initial geometry, at M06-2X/def2-TZVPP level of theory.

Figure S3. Optimized structures of $E_5^n\ (E = Si, Ge, Sn, Pb; n = -4, -2, 0)$ clusters from planar pentagon (D_{5h}) initial geometry, at M06-2X/def2-TZVPP level of theory.

Figure S4. Optimized structures of $E_5^n\ (E = Si, Ge, Sn, Pb; n = -4, -2, 0)$ clusters from square pyramid initial (C_{4v}) geometry, at BP86/def2-TZVPP level of theory.

Figure S5. Optimized structures of $E_5^n\ (E = Si, Ge, Sn, Pb; n = -4, -2, 0)$ clusters from trigonal bipyramid (D_{3h}) initial geometry, at BP86/def2-TZVPP level of theory.

Figure S6. Optimized structures of $E_5^n\ (E = Si, Ge, Sn, Pb; n = -4, -2, 0)$ clusters from planar pentagon (D_{5h}) initial geometry, at BP86/def2-TZVPP level of theory.

Figure S7. Optimized structures for $[Si_5\{Cr(CO)_3\}_2]^{4-}$ (a), $[Ge_5\{Cr(CO)_3\}_2]^{4-}$ (b), $[Sn_5\{Cr(CO)_3\}_2]^{4-}$ (c) and $[Pb_5\{Cr(CO)_3\}_2]^{4-}$ (d) complexes, at M06-2X/def2-TZVPP level of theory.

Figure S8. Optimized structures for $[Si_5\{Mo(CO)_3\}_2]^{4-}$ (a), $[Ge_5\{Mo(CO)_3\}_2]^{4-}$ (b), $[Sn_5\{Mo(CO)_3\}_2]^{4-}$ (c) and $[Pb_5\{Mo(CO)_3\}_2]^{4-}$ (d) complexes, at M06-2X/def2-TZVPP level of theory.

Figure S9. Optimized structures for $[Si_5\{W(CO)_3\}_2]^{4-}$ (a), $[Ge_5\{W(CO)_3\}_2]^{4-}$ (b), $[Sn_5\{W(CO)_3\}_2]^{4-}$ (c) and $[Pb_5\{W(CO)_3\}_2]^{4-}$ (d) complexes, at M06-2X/def2-TZVPP level of theory.

Figure S10. Four highest occupied molecular orbitals for $[Si_5\{Cr(CO)_3\}_2]^{4-}$ (a), $[Ge_5\{Cr(CO)_3\}_2]^{4-}$ (b), $[Sn_5\{Cr(CO)_3\}_2]^{4-}$ (c) and $[Pb_5\{Cr(CO)_3\}_2]^{4-}$ (d) complexes, at M06-2X/def2-TZVPP level of theory.

Figure S11. Four highest occupied molecular orbitals for $[Si_5\{Mo(CO)_3\}_2]^{4-}$ (a), $[Ge_5\{Mo(CO)_3\}_2]^{4-}$ (b), $[Sn_5\{Mo(CO)_3\}_2]^{4-}$ (c) and $[Pb_5\{Mo(CO)_3\}_2]^{4-}$ (d) complexes, at M06-2X/def2-TZVPP level of theory.

Figure S12. Four highest occupied molecular orbitals for $[Si_5\{W(CO)_3\}_2]^{4-}$ (a), $[Ge_5\{W(CO)_3\}_2]^{4-}$ (b), $[Sn_5\{W(CO)_3\}_2]^{4-}$ (c) and $[Pb_5\{W(CO)_3\}_2]^{4-}$ (d) complexes, at M06-2X/def2-TZVPP level of theory.

Figure S13. Deformation densities associated with the first four important orbital interactions for $[Si_5\{Cr(CO)_3\}_2]^{4-}$ (a), $[Ge_5\{Cr(CO)_3\}_2]^{4-}$ (b), $[Sn_5\{Cr(CO)_3\}_2]^{4-}$ (c) and $[Pb_5\{Cr(CO)_3\}_2]^{4-}$ (d) complexes, at BP86-D3/TZP(ZORA) level of theory.

Figure S14. Deformation densities associated with the first four important orbital interactions for $[Si_5\{Cr(CO)_3\}_2]^{4-}$ (a), $[Ge_5\{Mo(CO)_3\}_2]^{4-}$ (b), $[Sn_5\{Mo(CO)_3\}_2]^{4-}$ (c) and $[Pb_5\{Mo(CO)_3\}_2]^{4-}$ (d) complexes, at BP86-D3/TZP(ZORA) level of theory.

Figure S15. Deformation densities associated with the first four important orbital interactions for (a), $[Ge_5\{W(CO)_3\}_2]^{4-}$ (b), $[Sn_5\{W(CO)_3\}_2]^{4-}$ (c) and $[Pb_5\{W(CO)_3\}_2]^{4-}$ (d) complexes, at BP86-D3/TZP(ZORA) level of theory.

Figure S16. Optimized structures for $[Mo(CO)_6]$ (a), $[\eta^6\text{-}C_6H_6\{Mo(CO)_3\}]$ (b), $[Mes\{Mo(CO)_3\}]$ (c) and $[(\eta^5\text{-}C_5H_5)\{Mo(CO)_3\}_2]^-$ (d) complexes, at M06-2X/def2-TZVPP level of theory.

Table S1. Electronic energies (Hartree) for optimized structures for $E_5^n\,(E = Si, Ge, Sn, Pb; n = -4, -2, 0)$ clusters from different initial structures, at M06-2X/def2-TZVPP level of theory.

Initial structure	Cluster			
	Si_5	Ge_5	Sn_5	Pb_5
Square pyramid	−1447.3508614	−10385.1097046	−1071.3048338	−963.8448469
Triangular bipyramid	−1447.3508225	−10385.1097059	−1071.3048458	−963.8684009
Flat pentagon	−1447.3063576	−10385.0876782	−1071.2911033	−963.8621653
	Si_5^{2-}	Ge_5^{2-}	Sn_5^{2-}	Pb_5^{2-}
Square pyramid	−1447.3817545	−10385.1348706	−1071.3443037	−963.8851717
Triangular bipyramid	−1447.3816964	−10385.1348765	−1071.344277	−963.8851635
Flat pentagon	−1447.3121205	−10385.1348534	−1071.3442936	−963.8375353
	Si_5^{4-}	Ge_5^{4-}	Sn_5^{4-}	Pb_5^{4-}
Square pyramid	−1446.6881814	−10384.4266891	−1070.7848552	−963.315488
Triangular bipyramid	−1446.6881641	−10384.4266372	−1070.7743446	−963.3154976
Flat pentagon	−1446.6620006	−10384.4176391	failed	−963.3031012

Table S2. Electronic energies (Hartree) for optimized structures for $E_5^n\,(E = Si, Ge, Sn, Pb; n = -4, -2, 0)$ clusters from different initial structures, at BP86/def2-TZVPP level of theory.

Initial structure	Cluster			
	Si_5	Ge_5	Sn_5	Pb_5
Square pyramid	−1447.5894132	−10386.4547171	−1072.2995401	−965.3204571
Triangular bipyramid	−1447.5894190	−10386.4547196	−1072.2995408	−965.3427366
Flat pentagon	−1447.5494595	−10386.4313793	−1072.2814731	−965.3287632
	Si_5^{2-}	Ge_5^{2-}	Sn_5^{2-}	Pb_5^{2-}
Square pyramid	−1447.6141965	−10386.4641576	−1072.3384982	−965.3758572
Triangular bipyramid	−1447.6141969	−10386.4641581	−1072.3384672	−965.3758572
Flat pentagon	−1447.6141971	−10386.4176057	−1072.2954255	−965.3347756
	Si_5^{4-}	Ge_5^{4-}	Sn_5^{4-}	Pb_5^{4-}

Square pyramid	−1446.9366186	−10385.7555606	−1071.7922253	−964.8386400
Triangular bipyramid	−1446.9365943	−10385.7555436	−1071.7922253	failed
Flat pentagon	−1446.9261822	−10385.7611219	failed	−964.8328395

Table S3. The computed and experimental[a] E−E distances (Å) and E−E−E angles (°) for trigonal bipyramid $E^{2}{}_{5}^{-}$ $(E = Si, Ge, Sn, Pb)$ clusters, at M06−2X/def2-TZVPP level of theory.

	$Si^{2}{}_{5}^{-}$	$Ge^{2}{}_{5}^{-}$	$Sn^{2}{}_{5}^{-}$	$Pb^{2}{}_{5}^{-}$
distances				
E1–E2	2.36	2.54	2.92	3.05
	2.39	**2.48**	**2.90**	**3.00**
E1–E4	2.36	2.54	2.92	3.05
	2.34	**2.49**	**2.90**	**3.00**
E1–E5	2.36	2.54	2.92	3.05
	2.32	**2.51**	**2.90**	**3.00**
E2–E4	2.52	2.72	3.15	3.31
	2.51	**2.70**	**3.09**	**3.24**
E4–E5	2.52	2.72	3.15	3.31
	2.54	**2.68**	**3.09**	**3.24**
E2–E5	2.52	2.72	3.15	3.31
	2.56	**2.69**	**3.09**	**3.24**
E3–E2	2.36	2.54	2.92	3.05
	2.40	**2.47**	**2.83**	**3.00**
E3–E4	2.36	2.54	2.92	3.05
	2.35	**2.47**	**2.83**	**3.00**
E3–E5	2.36	2.54	2.92	3.05
	2.28	**2.49**	**2.83**	**3.00**
E3–E1	3.73	3.98	4.57	4.76
	3.66	**3.88**	**4.48**	**4.70**
RMS	*0.04*	*0.06*	*0.06*	*0.06*
Angles				
E1–E2–E3	104.08	103.40	102.95	102.54
	99.80	**102.66**	**102.83**	**102.99**
E1–E4–E3	104.07	103.35	102.91	102.57
	102.73	**101.91**	**102.84**	**102.99**
E1–E5–E3	104.07	103.31	102.91	102.57
	105.52	**103.26**	**102.84**	**102.99**
E5–E3–E2	64.39	64.96	65.33	65.60
	66.25	**66.19**	**64.44**	**65.25**
E5–E3–E4	64.36	64.94	65.27	65.60
	66.51	**65.84**	**64.44**	**65.25**

E2–E3–E4	64.39	64.95	65.33	65.60
	63.90	**65.35**	**64.44**	**65.25**
E5–E1–E2	64.39	64.97	65.33	65.60
	65.76	**65.76**	**66.31**	**65.28**
E5–E1–E4	64.36	64.96	65.27	65.60
	65.97	**65.36**	**66.31**	**65.25**
E2–E1–E4	64.39	64.96	65.33	65.60
	64.12	**64.81**	**66.31**	**65.25**
E4–E5–E2	60.02	59.98	60.03	60.00
	59.05	**59.59**	**60.00**	**60.00**
E5–E2–E4	59.97	60.01	59.95	60.00
	60.07	**60.08**	**60.00**	**60.00**
E2–E4–E5	60.01	60.01	60.03	60.00
	60.87	**60.32**	**60.00**	**60.00**
RMS	*1.75*	*0.51*	*0.66*	*0.33*

[a] The experimental data are given in bold.

Table S4. The computed and experimental[a] E−E distances (Å) and E−E−E angles (°) for trigonal bipyramid $E^{2}{}_{5}^{-}$ $(E = Si, Ge, Sn, Pb)$ clusters, at BP86/def2-TZVPP level of theory.

	$Si^{2}{}_{5}^{-}$	$Ge^{2}{}_{5}^{-}$	$Sn^{2}{}_{5}^{-}$	$Pb^{2}{}_{5}^{-}$
distances				
E1–E2	2.40	2.56	2.95	3.09
	2.39	**2.48**	**2.90**	**3.00**
E1–E4	2.40	2.56	2.95	3.10
	2.34	**2.49**	**2.90**	**3.00**
E1–E5	2.40	2.56	2.95	3.09
	2.32	**2.51**	**2.90**	**3.00**
E2–E4	2.57	2.76	3.16	3.30
	2.51	**2.70**	**3.09**	**3.24**
E4–E5	2.57	2.76	3.17	3.31
	2.54	**2.68**	**3.09**	**3.24**
E2–E5	2.57	2.76	3.16	3.30
	2.56	**2.69**	**3.09**	**3.24**
E3–E2	2.40	2.56	2.95	3.09
	2.40	**2.47**	**2.83**	**3.00**
E3–E4	2.40	2.56	2.95	3.09
	2.35	**2.47**	**2.83**	**3.00**
E3–E5	2.40	2.56	2.95	3.09
	2.28	**2.49**	**2.83**	**3.00**
E3–E1	3.76	4.00	4.62	4.87
	3.66	**3.88**	**4.48**	**4.70**
RMS	*0.06*	*0.08*	*0.09*	*0.09*
Angles				
E1–E2–E3	103.51	102.82	103.35	103.89
	99.80	**102.66**	**102.83**	**102.99**
E1–E4–E3	103.51	102.87	103.26	103.79
	102.73	**101.91**	**102.84**	**102.99**
E1–E5–E3	103.56	102.91	103.31	103.90
	105.52	**103.26**	**102.84**	**102.99**
E5–E3–E2	64.82	65.35	65.15	64.44
	66.25	**66.19**	**64.44**	**65.25**
E5–E3–E4	64.82	65.33	64.97	64.64

	66.51	**65.84**	**64.44**	**65.25**
E2–E3–E4	64.81	65.35	64.14	64.42
	63.90	**65.35**	**64.44**	**65.25**
E5–E1–E2	64.82	65.35	64.93	64.52
	65.76	**65.76**	**66.31**	**65.28**
E5–E1–E4	64.82	65.36	65.08	64.74
	65.97	**65.36**	**66.31**	**65.25**
E2–E1–E4	64.84	65.39	64.89	64.53
	64.12	**64.81**	**66.31**	**65.25**
E4–E5–E2	59.98	60.00	59.91	59.91
	59.05	**59.59**	**60.00**	**60.00**
E5–E2–E4	60.00	60.00	60.13	60.18
	60.07	**60.08**	**60.00**	**60.00**
E2–E4–E5	60.00	60.00	59.95	59.92
	60.87	**60.32**	**60.00**	**60.00**
RMS	*1.53*	*0.50*	*0.80*	*0.70*

[a] The experimental data are given in bold.

Table S5. Computed[a] and experimental structural parameters for $[Pb_5\{Mo(CO)_3\}_2]^{4-}$.

Distance	BP86	M06-2X	Exp.
Pb1–Pb2	3.11	3.10	3.02
Pb2–Pb3	3.13	3.10	3.06
Pb3–Pb4	3.13	3.09	3.06
Pb4–Pb5	3.13	3.09	3.05
Pb5–Pb1	3.13	3.10	3.01
Mo1–Mo2	3.33	3.33	3.22
Mo1–C1	1.95	1.92	1.93
Mo1–C2	1.95	1.92	1.92
Mo1–C3	1.95	1.92	1.96
Mo2–C4	1.95	1.92	1.92
Mo2–C5	1.95	1.92	1.93
Mo2–C6	1.95	1.92	1.93
RMS	*0.07*	*0.05*	–
C1–Mo1–C2	87.86	88.20	93.64
C1–Mo1–C3	86.92	87.36	89.23
C2–Mo1–C3	89.85	89.84	93.69
C4–Mo2–C5	86.91	87.36	87.56
C4–Mo2–C6	89.85	89.83	87.47
C5–Mo–C6	89.85	88.21	92.68
RMS	*3.36*	*3.50*	–
Mo1–Pb1–Mo2	64.33	63.24	63.43
Mo1–Pb2–Mo2	64.33	63.32	63.96
Mo1–Pb3–Mo2	63.55	63.04	63.63
Mo1–Pb4–Mo2	65.01	63.34	63.96
Mo1−Pb5−Mo2	63.55	63.05	63.67
RMS	*0.64*	*0.56*	–

[a] The data obtained at BP86/def2-TZVPP and M06-2X/def2-TZVPP levels of theory.

Table S6. Computed bond lengths (Å) for $[E_5\{Cr(CO)_3\}_2]^{4-}$ complexes (E=Si, Ge, Sn and Pb), at M06-2X/def2-TZVPP level of theory.

Bond lengths	$[Si_5\{Cr(CO)_3\}_2]^{4-}$	$[Ge_5\{Cr(CO)_3\}_2]^{4-}$	$[Sn_5\{Cr(CO)_3\}_2]^{4-}$	$[Pb_5\{Cr(CO)_3\}_2]^{4-}$
Cr1–E1	2.58	2.69	2.96	3.09
Cr1–E2	2.60	2.69	2.92	3.01
Cr1–E3	2.59	2.70	2.95	3.06
Cr1–E4	2.58	2.70	2.95	3.06
Cr1–E5	2.61	2.69	2.93	3.01
Cr2–E1	2.60	2.70	2.92	3.00
Cr2–E2	2.59	2.70	2.96	3.07
Cr2–E3	2.59	2.70	2.94	3.04
Cr2–E4	2.60	2.70	2.93	3.03
Cr2–E5	2.57	2.70	2.96	3.09
E1–E2	2.51	2.63	2.94	3.06
E2–E3	2.51	2.63	2.94	3.05
E3–E4	2.52	2.64	2.94	3.06
E4–E5	2.52	2.64	2.94	3.06
E5–E1	2.93	3.00	3.10	3.17

Table S7. Computed bond lengths (Å) for $[E_5\{Mo(CO)_3\}_2]^{4-}$ complexes (E=Si, Ge, Sn and Pb), at M06-2X/def2-TZVPP level of theory.

Bond lengths	$[Si_5\{Mo(CO)_3\}_2]^{4-}$	$[Ge_5\{Mo(CO)_3\}_2]^{4-}$	$[Sn_5\{Mo(CO)_3\}_2]^{4-}$	$[Pb_5\{Mo(CO)_3\}_2]^{4-}$
Mo1–E1	2.70	2.80	3.04	3.14
Mo1–E2	2.72	2.81	3.03	3.13
Mo1–E3	2.72	2.81	3.06	3.17
Mo1–E4	2.71	2.81	3.03	3.10
Mo1–E5	2.73	2.81	3.06	3.16
Mo2–E1	2.73	2.82	3.03	3.13
Mo2–E2	2.71	2.81	3.04	3.14
Mo2–E3	2.71	2.81	3.06	3.16
Mo2–E4	2.72	2.81	3.03	3.10
Mo2–E5	2.69	2.80	3.06	3.17
E1–E2	2.58	2.70	3.02	3.13
E2–E3	2.58	2.70	3.01	3.13
E3–E4	2.58	2.70	3.01	3.13
E4–E5	2.59	2.71	3.02	3.13
E5–E1	3.19	3.23	3.28	3.33

Table S8. Computed bond lengths (Å) for $[E_5\{W(CO)_3\}_2]^{4-}$ complexes (E=Si, Ge, Sn and Pb), at M06-2X/def2-TZVPP level of theory.

Bond lengths	$[Si_5\{W(CO)_3\}_2]^{4-}$	$[Ge_5\{W(CO)_3\}_2]^{4-}$	$[Sn_5\{W(CO)_3\}_2]^{4-}$	$[Pb_5\{W(CO)_3\}_2]^{4-}$
Mo1–E1	2.71	2.81	3.05	3.15
Mo1–E2	2.74	2.83	3.04	3.13
Mo1–E3	2.73	2.83	3.07	3.18
Mo1–E4	2.72	2.83	3.03	3.11
Mo1–E5	2.74	2.83	3.07	3.17
Mo2–E1	2.75	2.83	3.04	3.13
Mo2–E2	2.72	2.82	3.05	3.15

Mo2–E3	2.73	2.83	3.07	3.17
Mo2–E4	2.74	2.83	3.03	3.11
Mo2–E5	2.71	2.82	3.07	3.18
E1–E2	2.58	2.71	3.03	3.14
E2–E3	2.58	2.70	3.02	3.14
E3–E4	2.59	2.71	3.02	3.14
E4–E5	2.60	2.72	3.03	3.14
E5–E1	3.22	3.25	3.29	3.34

Table S9. Calculated values of uncorrected interaction energies between the fragments (IE, kcal/mol), for $[E_5\{M(CO)_3\}_2]^{4-}$; (E=Si, Ge, Sn and Pb; M=Cr, Mo and W) complexes, at M06-2X/def2-TZVPP level of theory.

Complex	$IE_{AB-A'}$	$IE_{A-BA'}$	IE_{A-B}	$IE_{B-A'}$	IE_{total}	
					(Eq. 6)	(Eq. 7)
$[Si_5\{Cr(CO)_3\}_2]^{4-}$	-209.7	-209.9	-196.4	-196.4	-406.1	-406.1
$[Ge_5\{Cr(CO)_3\}_2]^{4-}$	-208.4	-208.4	-186.5	-186.5	-394.9	-394.9
$[Sn_5\{Cr(CO)_3\}_2]^{4-}$	-174.6	-174.6	-125.5	-125.5	-300.1	-300.1
$[Pb_5\{Cr(CO)_3\}_2]^{4-}$	-157.3	-157.9	-124.7	-124.0	-281.9	-281.9
$[Si_5\{Mo(CO)_3\}_2]^{4-}$	-214.0	-213.9	-199.7	-199.8	-413.7	-413.7
$[Ge_5\{Mo(CO)_3\}_2]^{4-}$	-214.1	-214.1	-206.2	-206.3	-420.4	-420.4
$[Sn_5\{Mo(CO)_3\}_2]^{4-}$	-188.2	-188.0	-139.6	-139.7	-327.7	-327.7
$[Pb_5\{Mo(CO)_3\}_2]^{4-}$	-173.8	-174.4	-137.5	-136.9	-311.3	-311.3
$[Si_5\{W(CO)_3\}_2]^{4-}$	-233.0	-232.9	-218.4	-218.5	-451.4	-451.4
$[Ge_5\{W(CO)_3\}_2]^{4-}$	-233.5	-233.3	-221.9	-222.1	-455.4	-455.4
$[Sn_5\{W(CO)_3\}_2]^{4-}$	-204.7	-204.9	-156.3	-156.1	-361.0	-361.0
$[Pb_5\{W(CO)_3\}_2]^{4-}$	-197.2	-197.2	-161.7	-161.8	-358.9	-358.9

Table S10. Calculated values of uncorrected interaction energies between the fragments (IE, kcal/mol), for $[E_5\{M(CO)_3\}_2]^{4-}$; (E = Si, Ge, Sn and Pb; M = Cr, Mo and W) complexes, at BP86/def2-TZVPP level of theory.

Complex	$IE_{AB-A'}$	$IE_{A-BA'}$	IE_{A-B}	$IE_{B-A'}$	IE_{total}	
					(Eq. 6)	(Eq. 7)
$[Si_5\{Cr(CO)_3\}_2]^{4-}$	-238.8	-254.2	-178.9	-163.5	-417.7	-417.7
$[Ge_5\{Cr(CO)_3\}_2]^{4-}$	-254.9	-252.9	-170.8	-172.7	-425.7	-425.7
$[Sn_5\{Cr(CO)_3\}_2]^{4-}$	-193.8	-196.8	-131.8	-128.7	-325.5	-325.5

$[Pb_5\{Cr(CO)_3\}_2]^{4-}$	-179.7	-189.8	-127.3	-117.1	-306.9	-306.9
$[Si_5\{Mo(CO)_3\}_2]^{4-}$	-229.4	-230.6	-189.7	-188.4	-419.0	-419.0
$[Ge_5\{Mo(CO)_3\}_2]^{4-}$	-239.8	-234.5	-189.9	-195.1	-429.7	-429.7
$[Sn_5\{Mo(CO)_3\}_2]^{4-}$	-200.4	-196.5	-127.9	-131.8	-328.3	-328.3
$[Pb_5\{Mo(CO)_3\}_2]^{4-}$	-187.0	-192.3	-127.8	-122.6	-314.9	-314.9
$[Si_5\{W(CO)_3\}_2]^{4-}$	-247.8	-241.7	-200.3	-206.4	-448.1	-448.1
$[Ge_5\{W(CO)_3\}_2]^{4-}$	-245.3	-243.0	-211.9	-214.2	-457.2	-457.2
$[Sn_5\{W(CO)_3\}_2]^{4-}$	-210.7	-213.4	-146.3	-143.5	-357.0	-357.0
$[Pb_5\{W(CO)_3\}_2]^{4-}$	-199.8	-206.1	-140.8	-134.5	-340.6	-340.6

Table S11. Calculated values of corrected interaction energies between the fragments (IE, kcal/mol), for $[E_5\{M(CO)_3\}_2]^{4-}$; (E = Si, Ge, Sn and Pb; M = Cr, Mo and W) complexes, at BP86/def2-TZVPP level of theory.

Complex	$IE_{AB-A'}$	$IE_{A-BA'}$	IE_{A-B}	$IE_{B-A'}$	IE_{total}	
					(Eq. 6)	(Eq. 7)
$[Si_5\{Cr(CO)_3\}_2]^{4-}$	-195.8	-241.9	-148.3	-136.4	-372.1	-372.1
$[Ge_5\{Cr(CO)_3\}_2]^{4-}$	-196.8	-198.7	-134.5	-130.7	-362.1	-362.1
$[Sn_5\{Cr(CO)_3\}_2]^{4-}$	-179.7	-186.7	-114.6	-123.1	-305.9	-305.9
$[Pb_5\{Cr(CO)_3\}_2]^{4-}$	-162.1	-173.4	-103.0	-104.7	-289.3	-289.3
$[Si_5\{Mo(CO)_3\}_2]^{4-}$	-198.4	-209.4	-145.8	-147.0	-355.3	-355.3
$[Ge_5\{Mo(CO)_3\}_2]^{4-}$	-211.6	-203.2	-135.3	-140.7	-345.9	-345.9
$[Sn_5\{Mo(CO)_3\}_2]^{4-}$	-176.8	-179.2	-115.5	-119.4	-314.1	-314.1
$[Pb_5\{Mo(CO)_3\}_2]^{4-}$	-161.8	-166.9	-118.1	-110.4	-297.3	-297.3
$[Si_5\{W(CO)_3\}_2]^{4-}$	-232.6	-230.5	-171.6	-177.5	-411.5	-411.5
$[Ge_5\{W(CO)_3\}_2]^{4-}$	-223.5	-215.3	-178.0	-181.2	-402.4	-402.4
$[Sn_5\{W(CO)_3\}_2]^{4-}$	-209.5	-212.1	-139.4	-127.3	-340.7	-340.7
$[Pb_5\{W(CO)_3\}_2]^{4-}$	-191.7	-205.9	-129.4	-123.9	-326.8	-326.8

Table S12. Wiberg bond indices (WBIs) for $[E_5\{Cr(CO)_3\}_2]^{4-}$ at M06-2X/def2-TZVPP level of theory.

Bond	$[Si_5\{Cr(CO)_3\}_2]^{4-}$	$[Ge_5\{Cr(CO)_3\}_2]^{4-}$	$[Sn\{Cr(CO)_3\}_2]^{4-}$	$[Pb_5\{Cr(CO)_3\}_2]^{4-}$
Cr1–E1	0.47	0.47	0.42	0.39
Cr1–E2	0.44	0.45	0.46	0.48
Cr1–E3	0.45	0.46	0.44	0.43
Cr1–E4	0.46	0.46	0.43	0.42
Cr1–E5	0.43	0.45	0.47	0.48
Cr2–E1	0.43	0.45	0.47	0.49
Cr2–E2	0.46	0.46	0.43	0.40
Cr2–E3	0.45	0.46	0.45	0.46
Cr2–E4	0.44	0.45	0.45	0.46
Cr2–E5	0.43	0.47	0.43	0.40
E1–E2	0.61	0.61	0.62	0.63
E2–E3	0.62	0.62	0.62	0.62
E3–E4	0.62	0.62	0.62	0.63
E4–E5	0.61	0.61	0.62	0.63
E5–E1	0.60	0.61	0.61	0.62

Table S13. Wiberg bond indices (WBIs) for $[E_5\{Mo(CO)_3\}_2]^{4-}$ at M06-2X/def2-TZVPP level of theory.

Bond	$[Si_5\{Mo(CO)_3\}_2]^{4-}$	$[Ge_5\{Mo(CO)_3\}_2]^{4-}$	$[Sn\{Mo(CO)_3\}_2]^{4-}$	$[Pb_5\{Mo(CO)_3\}_2]^{4-}$
Mo1–E1	0.51	0.50	0.45	0.43
Mo1–E2	0.47	0.48	0.46	0.46
Mo1–E3	0.48	0.48	0.46	0.44
Mo1–E4	0.48	0.48	0.45	0.45
Mo1–E5	0.46	0.48	0.47	0.46
Mo2–E1	0.46	0.47	0.47	0.46
Mo2–E2	0.49	0.49	0.45	0.43
Mo2–E3	0.48	0.48	0.46	0.46
Mo2–E4	0.48	0.48	0.46	0.45
Mo2–E5	0.50	0.49	0.46	0.44
E1–E2	0.57	0.59	0.61	0.62
E2–E3	0.59	0.60	0.61	0.62
E3–E4	0.59	0.60	0.61	0.63
E4–E5	0.58	0.59	0.62	0.63
E5–E1	0.57	0.58	0.60	0.62

Table S14. Wiberg bond indices (WBIs) for $[E_5\{Cr(CO)_3\}_2]^{4-}$ at M06-2X/def2-TZVPP level of theory.

Bond	$[Si_5\{W(CO)_3\}_2]^{4-}$	$[Ge_5\{W(CO)_3\}_2]^{4-}$	$[Sn\{W(CO)_3\}_2]^{4-}$	$[Pb_5\{W(CO)_3\}_2]^{4-}$
W1–E1	0.53	0.52	0.47	0.45
W1–E2	0.49	0.49	0.48	0.47
W1–E3	0.49	0.49	0.47	0.46
W1–E4	0.50	0.50	0.47	0.46
W1–E5	0.48	0.48	0.48	0.47
W2–E1	0.47	0.48	0.47	0.47
W2–E2	0.51	0.51	0.47	0.45
W2–E3	0.49	0.49	0.48	0.47
W2–E4	0.49	0.49	0.47	0.46
W2–E5	0.52	0.51	0.47	0.46
E1–E2	0.57	0.57	0.58	0.60
E2–E3	0.58	0.58	0.58	0.58
E3–E4	0.59	0.59	0.58	0.59
E4–E5	0.58	0.58	0.58	0.59
E5–E1	0.56	0.56	0.57	0.58

Table S15. Calculated frequencies (cm^{-1})[a] for CO stretching bands in $[E_5\{Cr(CO)_3\}_2]^{4-}$ complexes as well as bond lengths (Å) and Wiberg bond indices (WBIs) for M-C and C-O bonds.

Complex	$\tilde{\upsilon}_{C=O}$	WBI				Distance(Å)			
$[Si_5\{Cr(CO)_3\}_2]^{4-}$	1661.95	Cr1–C1	1.31	Cr2-C4	1.31	Cr1-C1	1.792	Cr2-C4	1.792
		Cr1–C2	1.32	Cr2–C5	1.32	Cr1–C2	1.788	Cr2–C5	1.788
	1667.15	Cr1–C3	1.30	Cr2–C6	1.30	Cr1–C3	1.793	Cr2–C6	1.793
		C1–O1	1.81	C4–O4	1.81	C1–O1	1.183	C4–O4	1.183
	1734.89	C2–O2	1.80	C5–O5	1.80	C2–O2	1.184	C5–O5	1.184
		C3–O3	1.82	C6–O6	1.82	C3–O3	1.182	C6–O6	1.182
$[Ge_5\{Cr(CO)_3\}_2]^{4-}$	1656.68	Cr1–C1	1.33	Cr2–C4	1.32	Cr1–C1	1.788	Cr2-C4	1.789
		Cr1–C2	1.34	Cr2–C5	1.34	Cr1–C2	1.786	Cr2–C5	1.785
	1664.07	Cr1–C3	1.31	Cr2–C6	1.32	Cr1–C3	1.790	Cr2–C6	1.790
		C1–O1	1.80	C4–O4	1.80	C1–O1	1.184	C4–O4	1.183
	1732.73	C2–O2	1.80	C5–O5	1.79	C2–O2	1.184	C5–O5	1.184
		C3–O3	1.81	C6–O6	1.81	C3–O3	1.182	C6–O6	1.183
$[Sn_5\{Cr(CO)_3\}_2]^{4-}$	1663.21	Cr1–C1	1.36	Cr2–C4	1.36	Cr1–C1	1.787	Cr2–C4	1.789
		Cr1–C2	1.37	Cr2–C5	1.37	Cr1–C2	1.786	Cr2–C5	1.785
	1672.38	Cr1–C3	1.35	Cr2–C6	1.35	Cr1–C3	1.790	Cr2–C6	1.790

		C1–O1	1.80	C4–O4	1.81	C1–O1	1.182	C4–O4	1.181
	1734.48	C2–O2	1.79	C5–O5	1.79	C2–O2	1.182	C5–O5	1.183
		C3–O3	1.81	C6–O6	1.81	C3–O3	1.180	C6–O6	1.180
	1640.40	Cr1–C1	1.38	Cr2–C4	1.37	Cr1–C1	1.784	Cr2–C4	1.786
		Cr1–C2	1.39	Cr2–C5	1.39	Cr1–C2	1.783	Cr2–C5	1.782
$[Pb_5\{Cr(CO)_3\}_2]^{4-}$	1652.32	Cr1–C3	1.37	Cr2–C6	1.38	Cr1–C3	1.787	Cr2–C6	1.785
		C1–O1	1.78	C4–O4	1.79	C1–O1	1.185	C4–O4	1.183
	1716.33	C2–O2	1.78	C5–O5	1.77	C2–O2	1.185	C5–O5	1.186
		C3–O3	1.80	C6–O6	1.79	C3–O3	1.182	C6–O6	1.183

[a] The scaling factor λ=0.9323 was used at M06-2X/def2-TZVPP level of theory.

Table S16. Calculated frequencies (cm^{-1})[a] for CO stretching bands in $[E_5\{Mo(CO)_3\}_2]^{4-}$ complexes as well as bond lengths (Å) and Wiberg bond indices (WBIs) for M-C and C-O bonds.

Complex	$\bar{\upsilon}_{C=O}$	WBI				Distance(Å)			
	1691.30	Mo1–C1	1.34	Mo2–C4	1.33	Mo1–C1	1.946	Mo2–C4	1.948
		Mo1–C2	1.36	Mo2–C5	1.36	Mo1–C2	1.944	Mo2–C5	1.942
$[Si_5\{Mo(CO)_3\}_2]^{4-}$	1699.1	Mo1–C3	1.32	Mo2–C6	1.32	Mo1–C3	1.948	Mo2–C6	1.948
		C1–O1	1.82	C4–O4	1.83	C1–O1	1.177	C4–O4	1.176
	1771.38	C2–O2	1.82	C5–O5	1.81	C2–O2	1.179	C5–O5	1.179
		C3–O3	1.84	C6–O6	1.84	C3–O3	1.175	C6–O6	1.176
	1686.66	Mo1–C1	1.37	Mo2–C4	1.36	Mo1–C1	1.938	Mo2–C4	1.939
		Mo1–C2	1.38	Mo2–C5	1.39	Mo1–C2	1.936	Mo2–C5	1.934
$[Ge_5\{Mo(CO)_3\}_2]^{4-}$	1696.01	Mo1–C3	1.35	Mo2–C6	1.36	Mo1–C3	1.939	Mo2–C6	1.939
		C1–O1	1.82	C4–O4	1.83	C1–O1	1.178	C4–O4	1.177
	1770.38	C2–O2	1.81	C5–O5	1.81	C2–O2	1.179	C5–O5	1.180
		C3–O3	1.83	C6–O6	1.83	C3–O3	1.176	C6–O6	1.177
$[Sn_5\{Mo(CO)_3\}_2]^{4-}$	1691.49	Mo1–C1	1.40	Mo2–C4	1.40	Mo1–C1	1.930	Mo2–C4	1.930
		Mo1–C2	1.43	Mo2–C5	1.42	Mo1–C2	1.927	Mo2–C5	1.928

	1701.74	Mo1–C3	1.40	Mo2–C6	1.41	Mo1–C3	1.930	Mo2–C6	1.929
		C1–O1	1.83	C4–O4	1.83	C1–O1	1.176	C4–O4	1.176
	1773.98	C2–O2	1.81	C5–O5	1.81	C2–O2	1.179	C5–O5	1.178
		C3–O3	1.82	C6–O6	1.82	C3–O3	1.176	C6–O6	1.177
	1668.65	Mo1–C1	1.45	Mo2–C4	1.43	Mo1–C1	1.920	Mo2–C4	1.921
		Mo1–C2	1.45	Mo2–C5	1.45	Mo1–C2	1.920	Mo2–C5	1.919
$[Pb_5\{Mo(CO)_3\}_2]^{4-}$	1681.00	Mo1–C3	1.43	Mo2–C6	1.44	Mo1–C3	1.920	Mo2–C6	1.920
		C1–O1	1.79	C4–O4	1.81	C1–O1	1.182	C4–O4	1.179
	1758.11	C2–O2	1.79	C5–O5	1.79	C2–O2	1.181	C5–O5	1.182
		C3–O3	1.81	C6–O6	1.80	C3–O3	1.179	C6–O6	1.180

[a] The scaling factor λ=0.9323 was used at M06-2X/def2-TZVPP level of theory.

Table S17. Calculated frequencies (cm^{-1})[a] for CO stretching bands in $[E_5\{W(CO)_3\}_2]^{4-}$ complexes as well as bond lengths (Å) and Wiberg bond indices (WBIs) for M-C and C-O bonds.

Complex	$\bar{\upsilon}_{C=O}$	WBI				Distance(Å)			
	1690.99	W1–C1	1.32	W 2–C4	1.31	W1–C1	1.966	W 2–C4	1.968
		W1–C2	1.34	W2–C5	1.35	W1–C2	1.963	W2–C5	1.961
$[Si_5\{W(CO)_3\}_2]^{4-}$	1699.85	W1–C3	1.30	W2–C6	1.30	W1–C3	1.968	W2–C6	1.968
		C1–O1	1.79	C4–O4	1.80	C1–O1	1.179	C4–O4	1.177
	1771.58	C2–O2	1.78	C5–O5	1.78	C2–O2	1.180	C5–O5	1.181
		C3–O3	1.81	C6–O6	1.81	C3–O3	1.177	C6–O6	1.177
	1683.94	W1–C1	1.36	W 2–C4	1.34	W1–C1	1.958	W 2–C4	1.960
		W1–C2	1.37	W2–C5	1.38	W1–C2	1.956	W2–C5	1.954
$[Ge_5\{W(CO)_3\}_2]^{4-}$	1693.31	W1–C3	1.34	W2–C6	1.34	W1–C3	1.960	W2–C6	1.960
		C1–O1	1.78	C4–O4	1.79	C1–O1	1.180	C4–O4	1.179
	1767.64	C2–O2	1.78	C5–O5	1.77	C2–O2	1.181	C5–O5	1.182
		C3–O3	1.80	C6–O6	1.79	C3–O3	1.178	C6–O6	1.179
$[Sn_5\{W(CO)_3\}_2]^{4-}$	1690.37	W1–C1	1.41	W 2–C4	1.40	W1–C1	1.950	W 2–C4	1.951
		W1–C2	1.43	W2–C5	1.43	W1–C2	1.949	W2–C5	1.948

	1699.49	W1–C3	1.39	W2–C6	1.41	W1–C3	1.951	W2–C6	1.950
		C1–O1	1.79	C4–O4	1.80	C1–O1	1.179	C4–O4	1.177
	1770.97	C2–O2	1.78	C5–O5	1.78	C2–O2	1.180	C5–O5	1.180
		C3–O3	1.80	C6–O6	1.79	C3–O3	1.177	C6–O6	1.178
	1670.53	W1–C1	1.44	W 2–C4	1.44	W1–C1	1.942	W 2–C4	1.942
		W1–C2	1.46	W2–C5	1.44	W1–C2	1.940	W2–C5	1.942
$[Pb_5\{W(CO)_3\}_2]^{4-}$	1683.14	W1–C3	1.44	W2–C6	1.46	W1–C3	1.942	W2–C6	1.940
		C1–O1	1.77	C4–O4	1.77	C1–O1	1.182	C4–O4	1.181
	1756.67	C2–O2	1.75	C5–O5	1.77	C2–O2	1.184	C5–O5	1.182
		C3–O3	1.75	C6–O6	1.76	C2–O2	1.182	C5–O5	1.181

[a] The scaling factor λ=0.9323 was used at M06-2X/def2-TZVPP level of theory.

Table S18. Energy decomposition analysis results between $[E_5\{M(CO)_3\}]^{4-}$ and {M(CO)$_3$} fragments (A−BA') in $[E_5\{M(CO)_3\}_2]^{4-}$ *complexes* (E=Si, Ge, Sn and Pb; M=Cr, Mo and W) at BP86-D3/TZP(ZORA) level of theory.

Complex	ΔE_{int}	ΔE_{Pauli}	ΔE_{elstat}	ΔE_{orb}	ΔE_{disp}
$[Si_5\{Cr(CO)_3\}_2]^{4-}$	−233.2	410.8	−315.5 (49%)	−322.6 (50%)	−5.9 (1%)
$[Ge_5\{Cr(CO)_3\}_2]^{4-}$	−202.0	326.3	−269.0 (51%)	−252.4 (48%)	−6.9 (1%)
$[Sn_5\{Cr(CO)_3\}_2]^{4-}$	−182.4	323.5	−252.2 (50%)	−245.8 (49%)	−8.0 (2%)
$[Pb_5\{Cr(CO)_3\}_2]^{4-}$	−163.0	285.7	−229.1 (51%)	−209.8 (47%)	−9.7 (2%)
$[Si_5\{Mo(CO)_3\}_2]^{4-}$	−217.2	349.8	−291.1 (51%)	−269.2 (47%)	−6.7 (1%)
$[Ge_5\{Mo(CO)_3\}_2]^{4-}$	−194.1	301.1	−262.0 (53%)	−226.0 (46%)	−7.3 (1%)
$[Sn_5\{Mo(CO)_3\}_2]^{4-}$	−178.3	351.0	−284.5 (54%)	−236.9 (45%)	−7.9 (2%)
$[Pb_5\{Mo(CO)_3\}_2]^{4-}$	−164.9	309.3	−257.6 (54%)	−206.9 (44%)	−9.7 (2%)
$[Si_5\{W(CO)_3\}_2]^{4-}$	−227.1	315.7	−290.9 (54%)	−244.7 (45%)	−7.2 (1%)
$[Ge_5\{W(CO)_3\}_2]^{4-}$	−223.6	394.5	−340.6 (55%)	−269.7 (44%)	−7.8 (1%)
$[Sn_5\{W(CO)_3\}_2]^{4-}$	−199.1	398.7	−328.9 (55%)	−260.6 (44%)	−8.3 (1%)
$[Pb_5\{W(CO)_3\}_2]^{4-}$	−185.7	353.8	−302.3 (56%)	−227.1 (42%)	−10.1 (2%)

Table S19. Comparison of computed Ge−Ge distances (Å) for trigonal bipyramid Ge^{2-}_5 cluster in Ref. 43 and in this study.

Distances (Å)	Ref. 43	This study	
	B3LYP/LANL2DZ	BP86/def2-TZVPP	M06-2X/def2-TZVPP
Ge1—Ge4	2.577	2.558	2.536
Ge1—Ge5	2.577	2.559	2.536
Ge2—Ge4	2.577	2.558	2.536
Ge2—Ge5	2.577	2.557	2.537
Ge3—Ge4	2.577	2.558	2.537
Ge3—Ge5	2.577	2.556	2.538
Ge1—Ge2	2.818	2.762	2.724
Ge1—Ge3	2.818	2.762	2.724
Ge2—Ge3	2.818	2.761	2.724
Ge4...Ge5	3.997	4.000	3.980
RMS	0.107	0.080	0.060

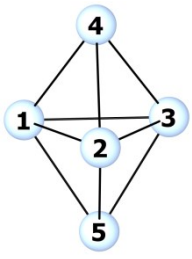

Table S20. Comparison of computed Ge−Ge distances (Å) for trigonal bipyramid Ge_5 cluster in Ref. 43 and in this study.

Distances (Å)	Ref. 43	This study	
	B3LYP/LANL2DZ	BP86/def2-TZVPP	M06-2X/def2-TZVPP
Ge1—Ge4	2.491	2.464	2.458
Ge1—Ge5	2.491	2.464	2.458
Ge2—Ge4	2.491	2.464	2.458
Ge2—Ge5	2.491	2.464	2.457
Ge3—Ge4	2.491	2.464	2.458
Ge3—Ge5	2.491	2.464	2.457
Ge1...Ge2	3.351	3.284	3.281
Ge1...Ge3	3.351	3.284	3.280
Ge2...Ge3	3.351	3.284	3.280
Ge4—Ge5	3.141	3.147	3.133
RMS	There is not experimental data for comparison		

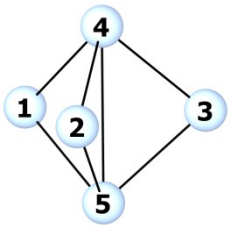

n	Si_5^n	Ge_5^n	Sn_5^n	Pb_5^n
0	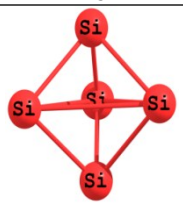	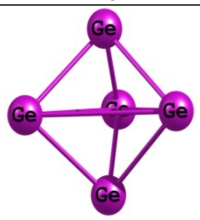	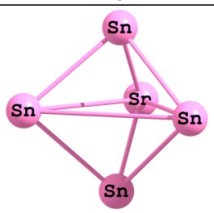	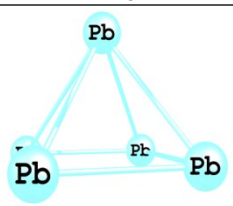

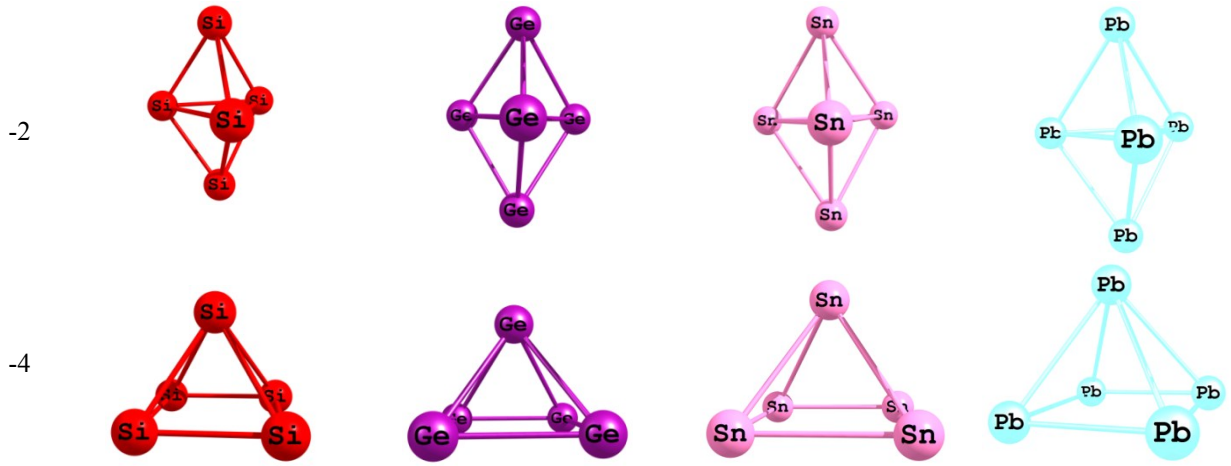

Figure S1. Optimized structures of E_5^n $(E = Si, Ge, Sn, Pb; n = -4, -2, 0)$ clusters from square pyramid initial (C_{4v}) geometry, at M06-2X/def2-TZVPP level of theory.

n	Si_5^n	Ge_5^n	Sn_5^n	Pb_5^n
0				
-2				
-4				

Figure S2. Optimized structures of E_5^n $(E = Si, Ge, Sn, Pb; n = -4, -2, 0)$ clusters from trigonal bipyramid (D_{3h}) initial geometry, at M06-2X/def2-TZVPP level of theory.v

n	Si_5^n	Ge_5^n	Sn_5^n	Pb_5^n

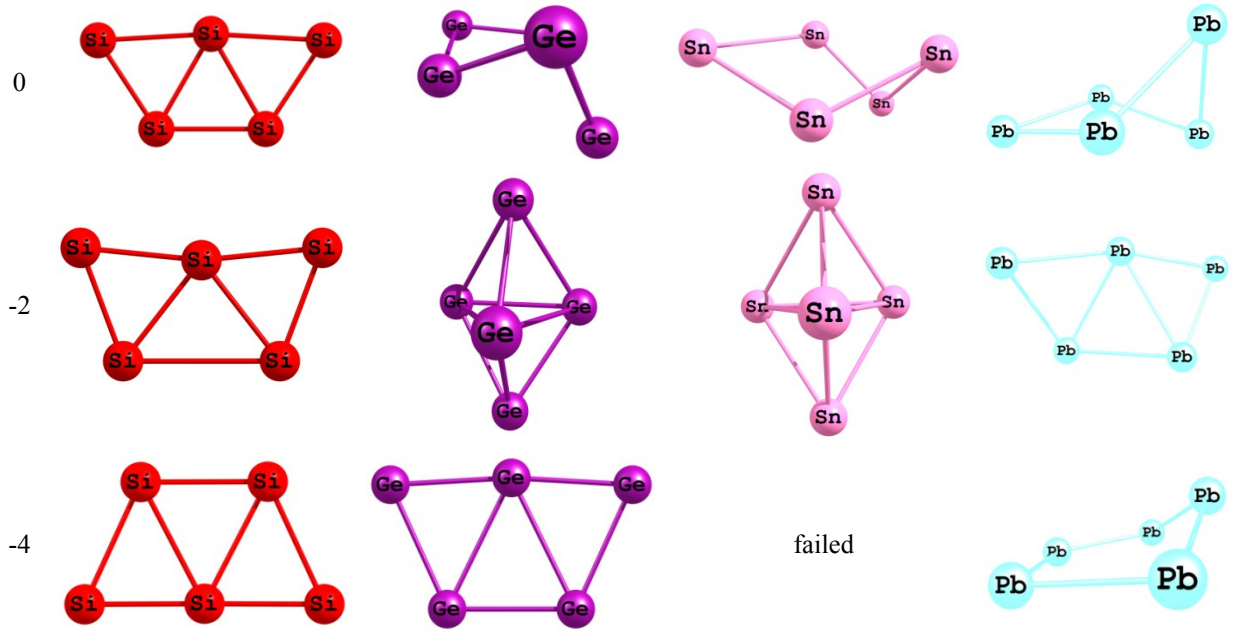

Figure S3. Optimized structures of $E_5^n\ (E = Si, Ge, Sn, Pb; n = -4, -2, 0)$ clusters from planar pentagon (D_{5h}) initial geometry, at M06-2X/def2-TZVPP level of theory.

n	Si_5^n	Ge_5^n	Sn_5^n	Pb_5^n
0				
-2				
-4				

Figure S4. Optimized structures of $E_5^n\ (E = Si, Ge, Sn, Pb; n = -4, -2, 0)$ clusters from square pyramid (C_{4v}) initial geometry, at BP86/def2-TZVPP level of theory.

n	Si_5^n	Ge_5^n	Sn_5^n	Pb_5^n

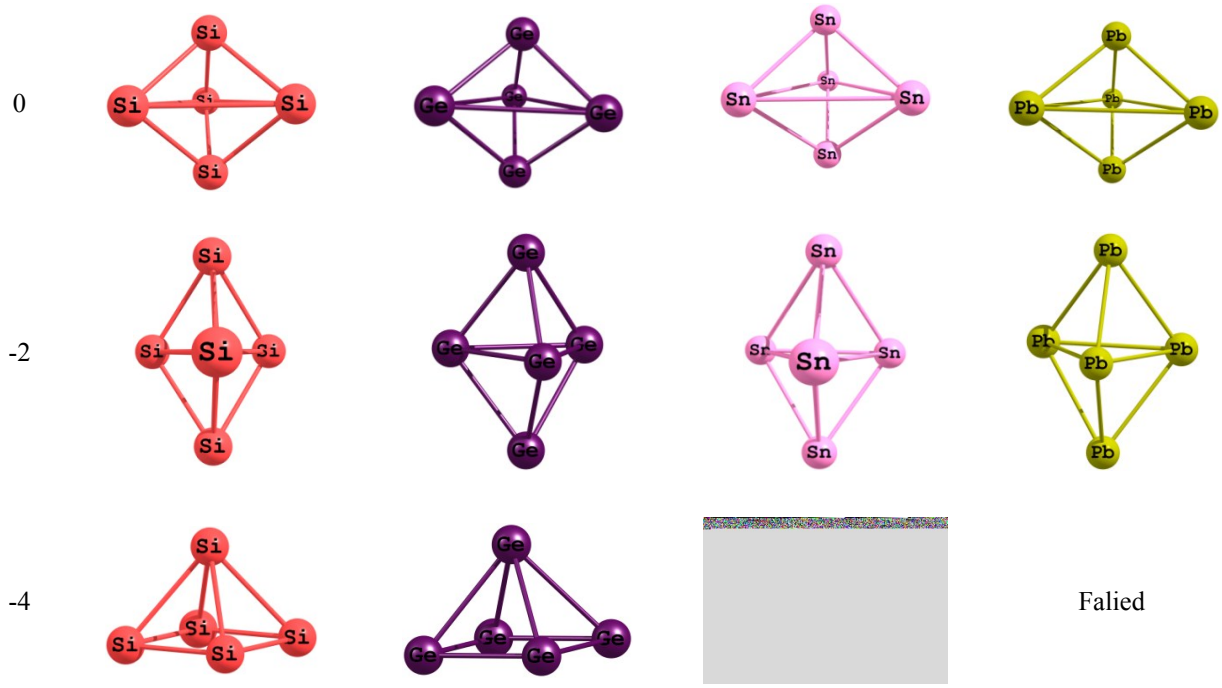

Figure S5. Optimized structures of $E_5^n\,(E = Si, Ge, Sn, Pb; n = -4, -2, 0)$ clusters from trigonal bipyramid (D_{3h}) initial geometry, at BP86/def2-TZVPP level of theory.

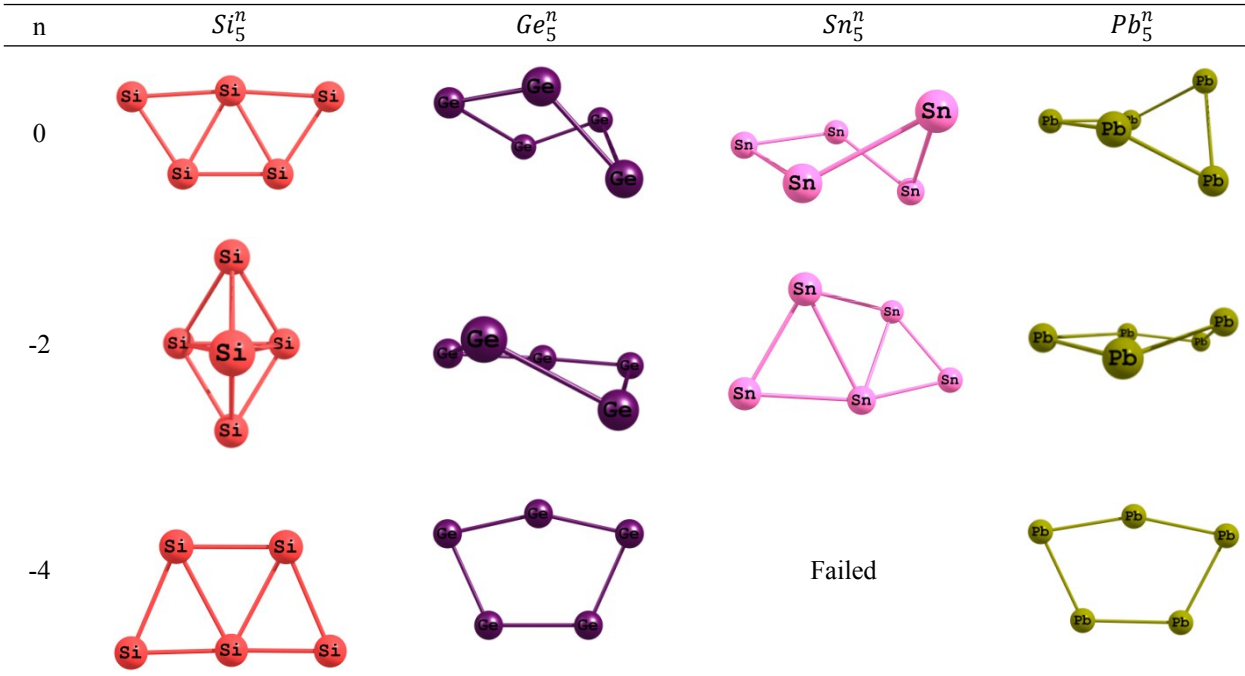

Figure S6. Optimized structures of $E_5^n\,(E = Si, Ge, Sn, Pb; n = -4, -2, 0)$ clusters from planar pentagon (D_{5h}) initial geometry, at BP86/def2-TZVPP level of theory.

(a)

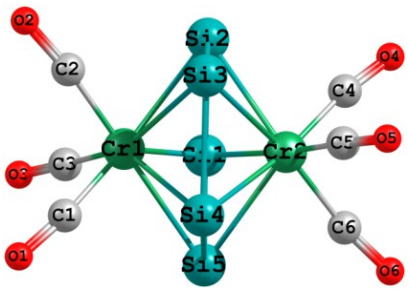

side view

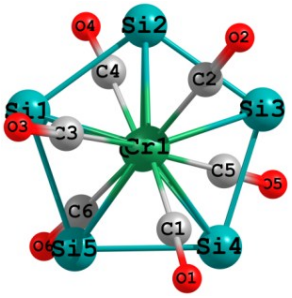

top view

(b)

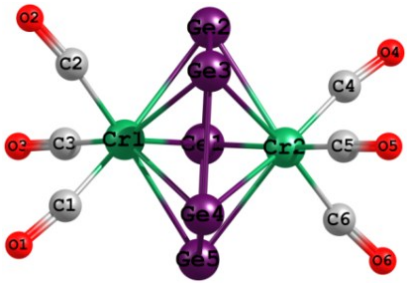

side view

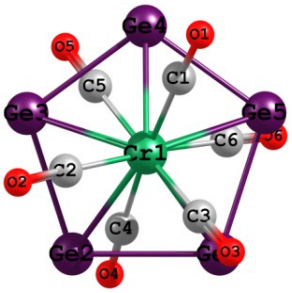

top view

(c)

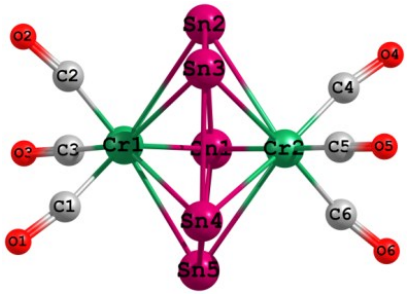

side view

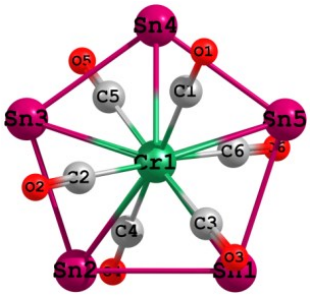

top view

(d)

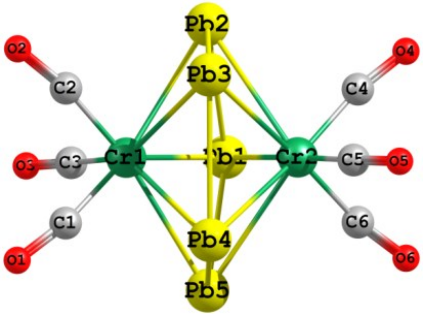

side view

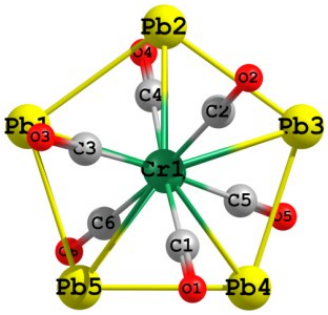

top view

Figure S7. Optimized structures for $[Si_5\{Cr(CO)_3\}_2]^{4-}$ (a), $[Ge_5\{Cr(CO)_3\}_2]^{4-}$ (b), $[Sn_5\{Cr(CO)_3\}_2]^{4-}$ (c) and $[Pb_5\{Cr(CO)_3\}_2]^{4-}$ (d) complexes, at M06-2X/def2-TZVPP level of theory.

(a)

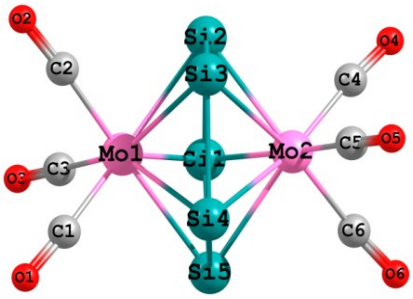

side view

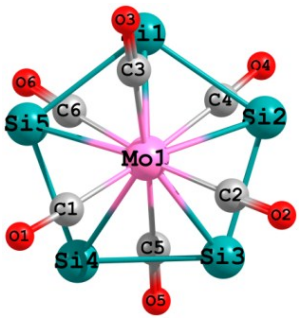

top view

(b)

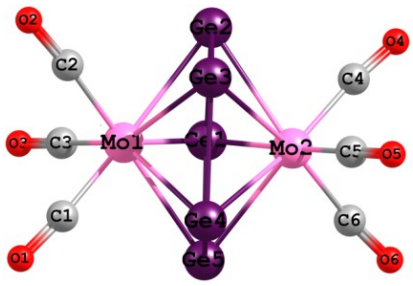

side view

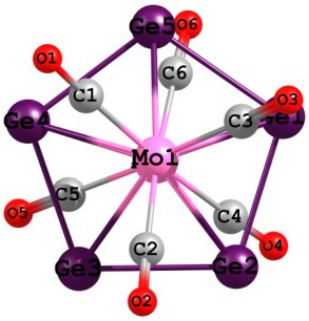

top view

(c)

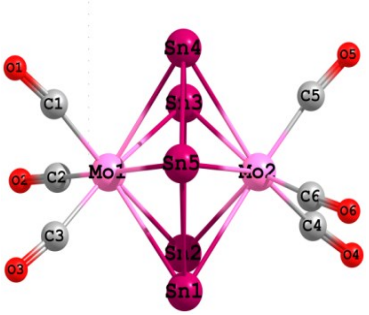

side view

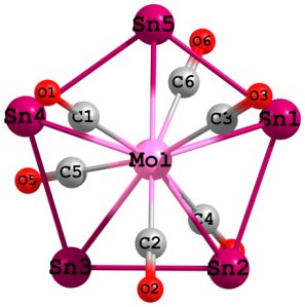

top view

(d)

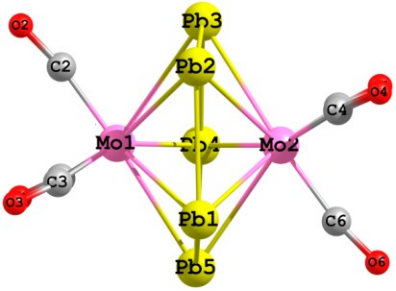

side view

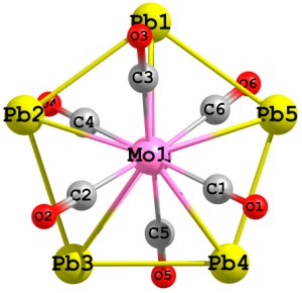

top view

Figure S8. Optimized structures for $[Si_5\{Mo(CO)_3\}_2]^{4-}$ (a), $[Ge_5\{Mo(CO)_3\}_2]^{4-}$ (b), $[Sn_5\{Mo(CO)_3\}_2]^{4-}$ (c) and $[Pb_5\{Mo(CO)_3\}_2]^{4-}$ (d) complexes, at M06-2X/def2-TZVPP level of theory.

(a)

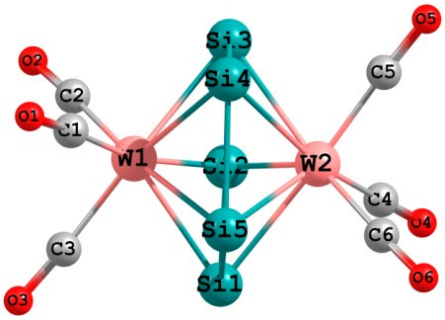

side view

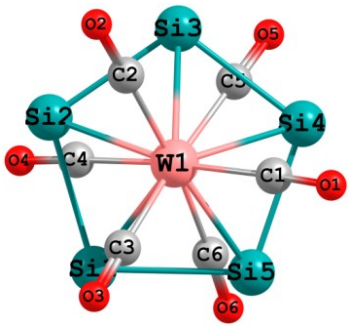

top view

(b)

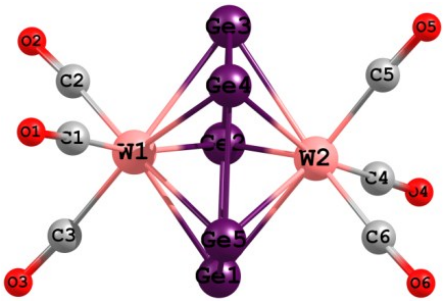

side view

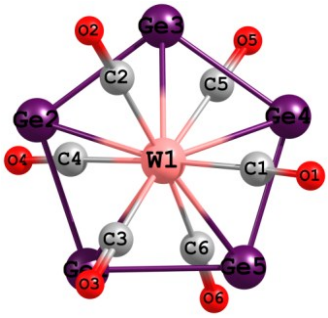

top view

(c)

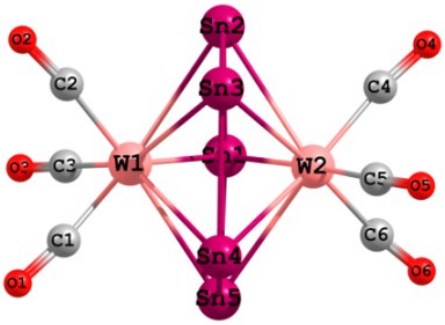

side view

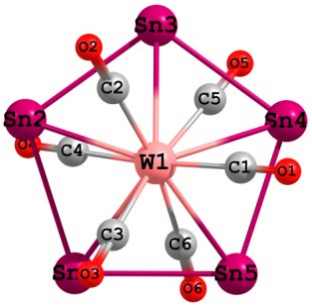

top view

(d)

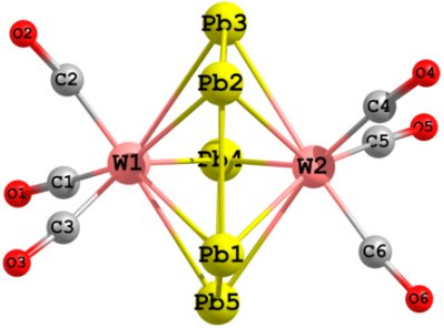

side view

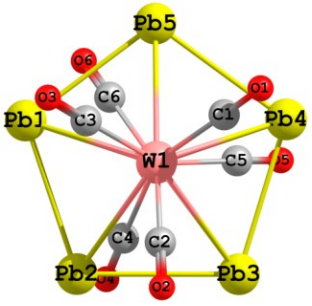

top view

Figure S9. Optimized structures for $[Si_5\{W(CO)_3\}_2]^{4-}$ (a), $[Ge_5\{W(CO)_3\}_2]^{4-}$ (b), $[Sn_5\{W(CO)_3\}_2]^{4-}$ (c) and $[Pb_5\{W(CO)_3\}_2]^{4-}$ (d) complexes, at M06-2X/def2-TZVPP level of theory.

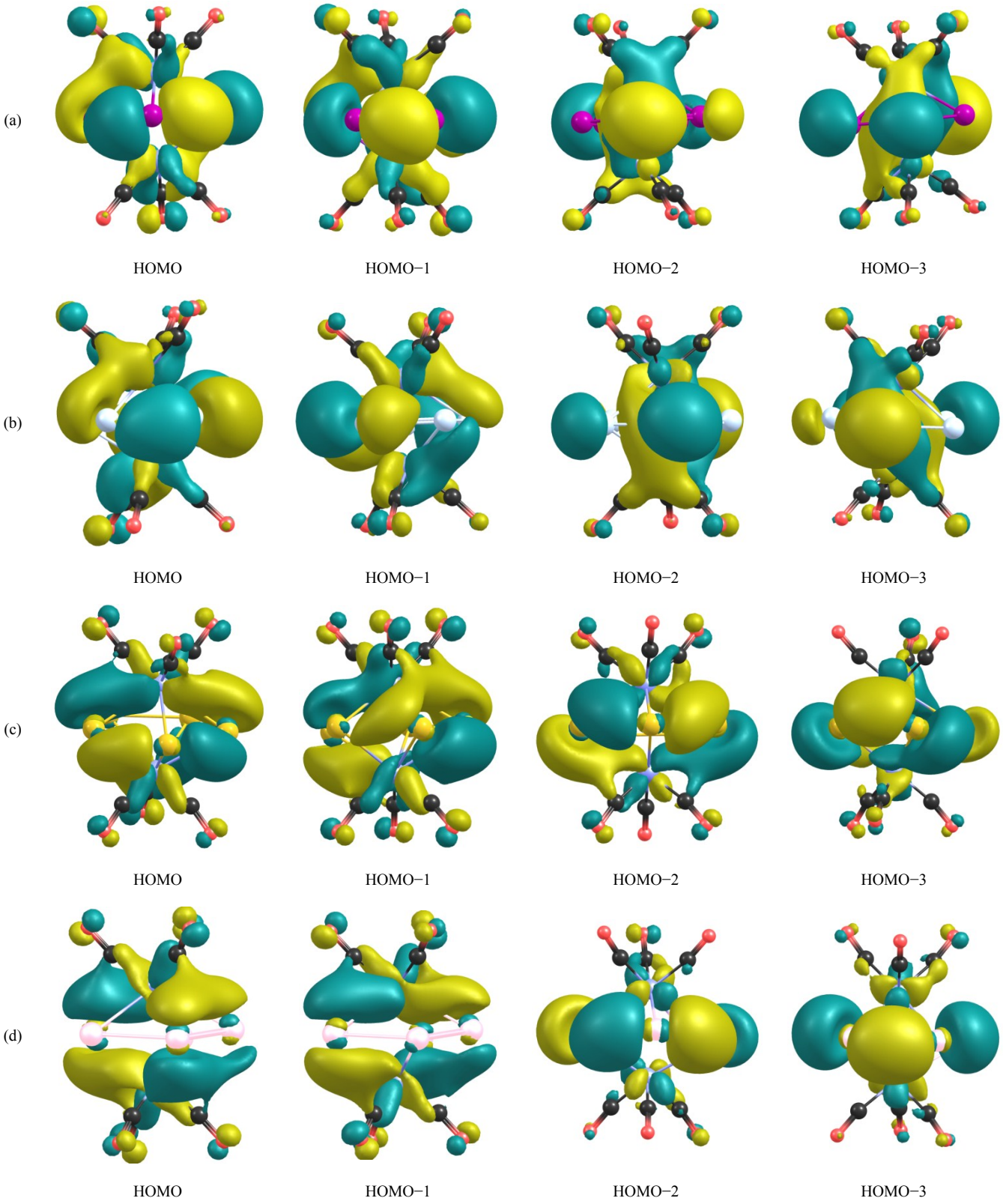

Figure S10. Four highest occupied molecular orbitals for $[Si_5\{Cr(CO)_3\}_2]^{4-}$ (a), $[Ge_5\{Cr(CO)_3\}_2]^{4-}$ (b), $[Sn_5\{Cr(CO)_3\}_2]^{4-}$ (c) and $[Pb_5\{Cr(CO)_3\}_2]^{4-}$ (d) complexes, at M06-2X/def2-TZVPP level of theory.

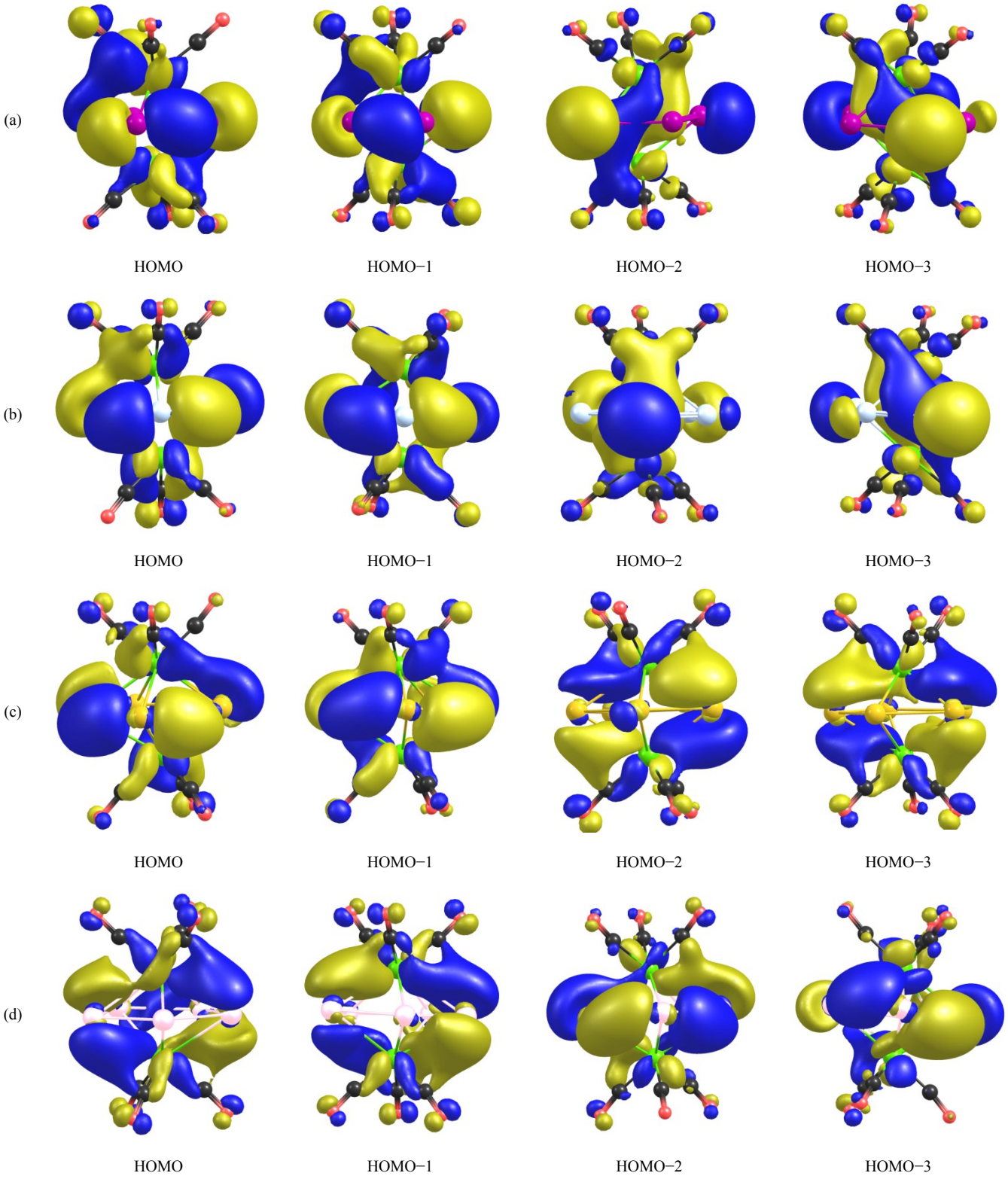

Figure S11. Four highest occupied molecular orbitals for $[Si_5\{Mo(CO)_3\}_2]^{4-}$ (a), $[Ge_5\{Mo(CO)_3\}_2]^{4-}$ (b), $[Sn_5\{Mo(CO)_3\}_2]^{4-}$ (c) and $[Pb_5\{Mo(CO)_3\}_2]^{4-}$ (d) complexes, at M06-2X/def2-TZVPP level of theory.

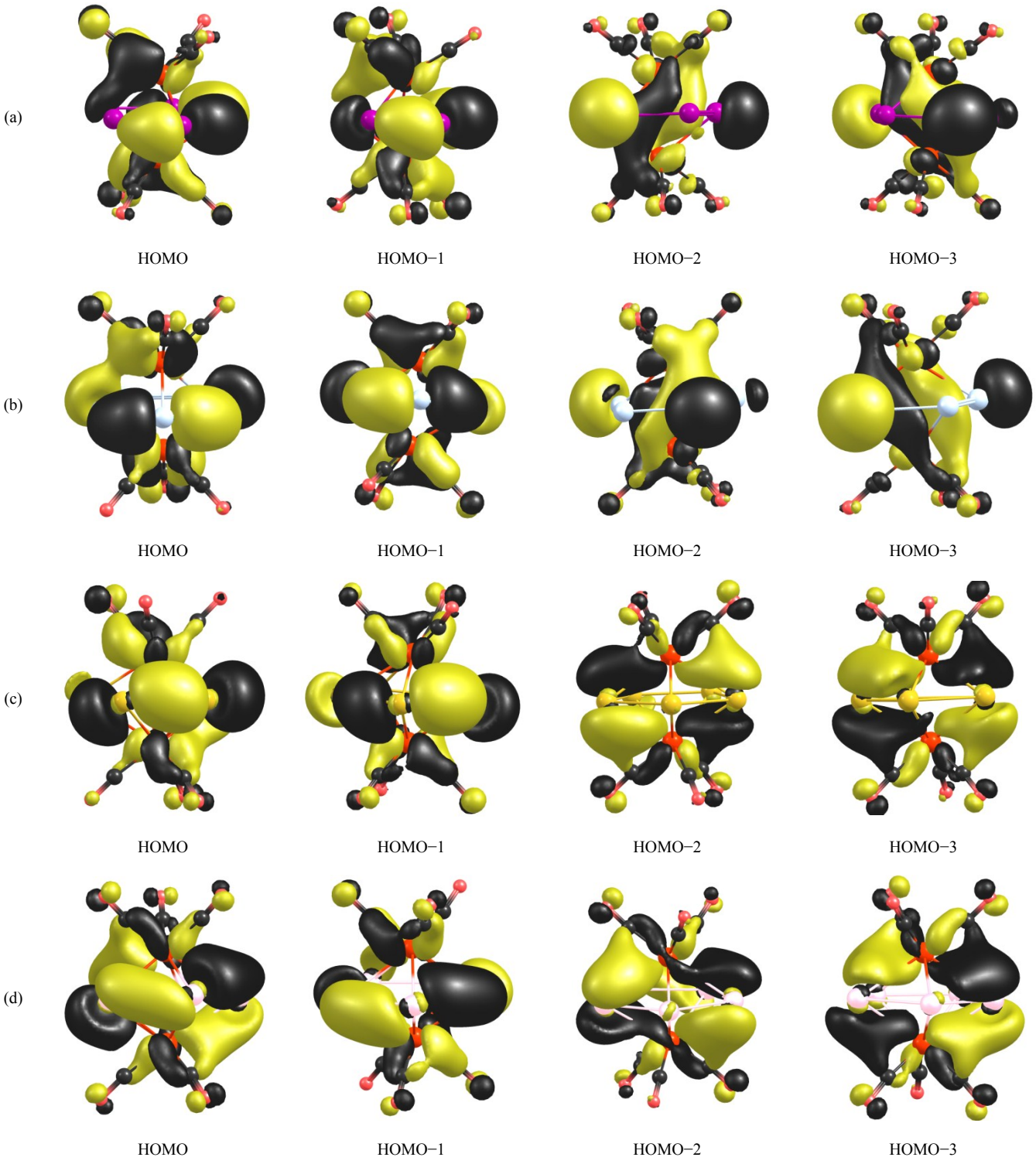

Figure S12. Four highest occupied molecular orbitals for $[Si_5\{W(CO)_3\}_2]^{4-}$ (a), $[Ge_5\{W(CO)_3\}_2]^{4-}$ (b), $[Sn_5\{W(CO)_3\}_2]^{4-}$ (c) and $[Pb_5\{W(CO)_3\}_2]^{4-}$ (d) complexes, at M06-2X/def2-TZVPP level of theory.

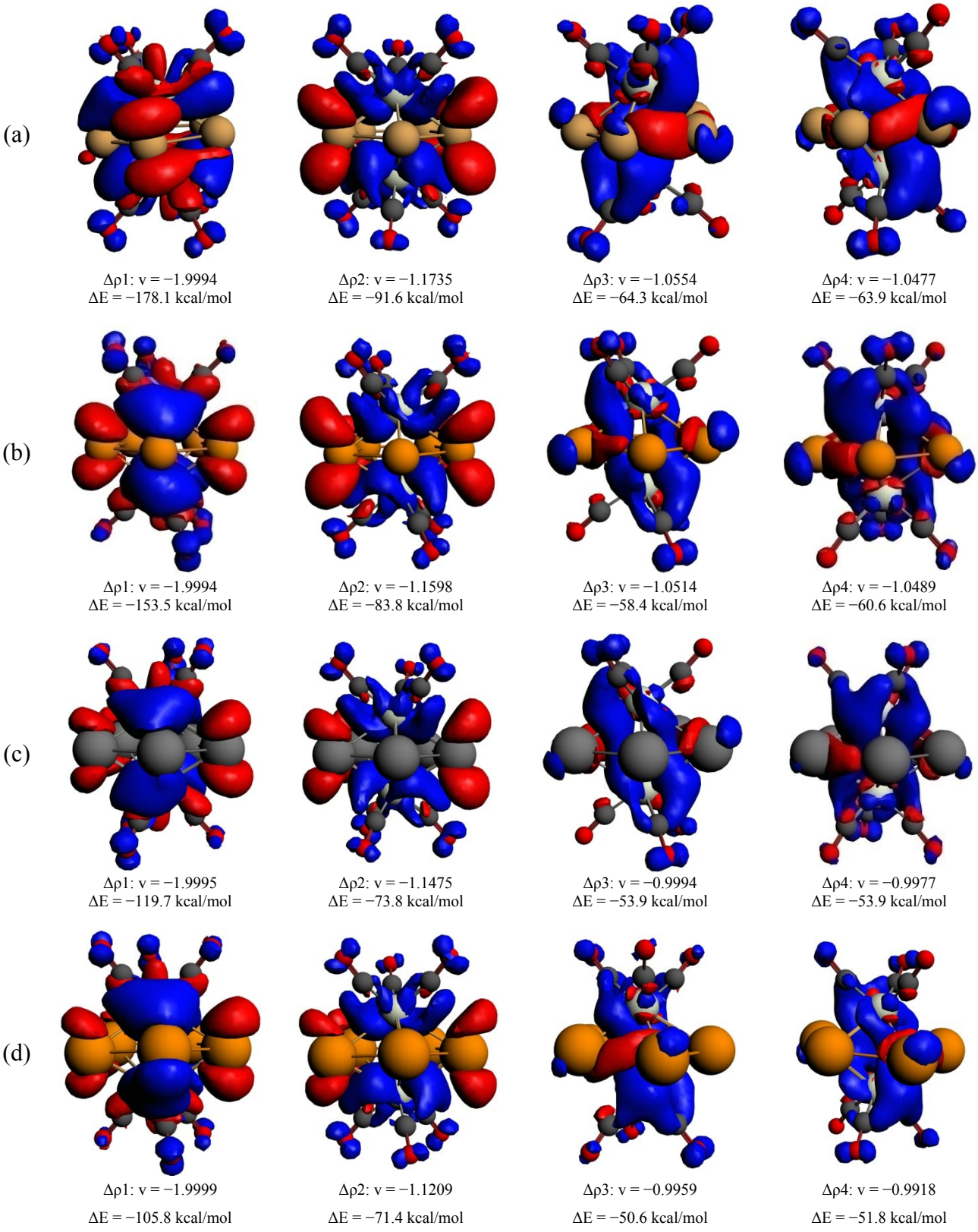

Figure S13. Deformation densities associated with the first four important orbital interactions for $[Si_5\{Cr(CO)_3\}_2]^{4-}$ (a), $[Ge_5\{Cr(CO)_3\}_2]^{4-}$ (b), $[Sn_5\{Cr(CO)_3\}_2]^{4-}$ (c) and $[Pb_5\{Cr(CO)_3\}_2]^{4-}$ (d) complexes, at BP86-D3/TZP(ZORA) level of theory.

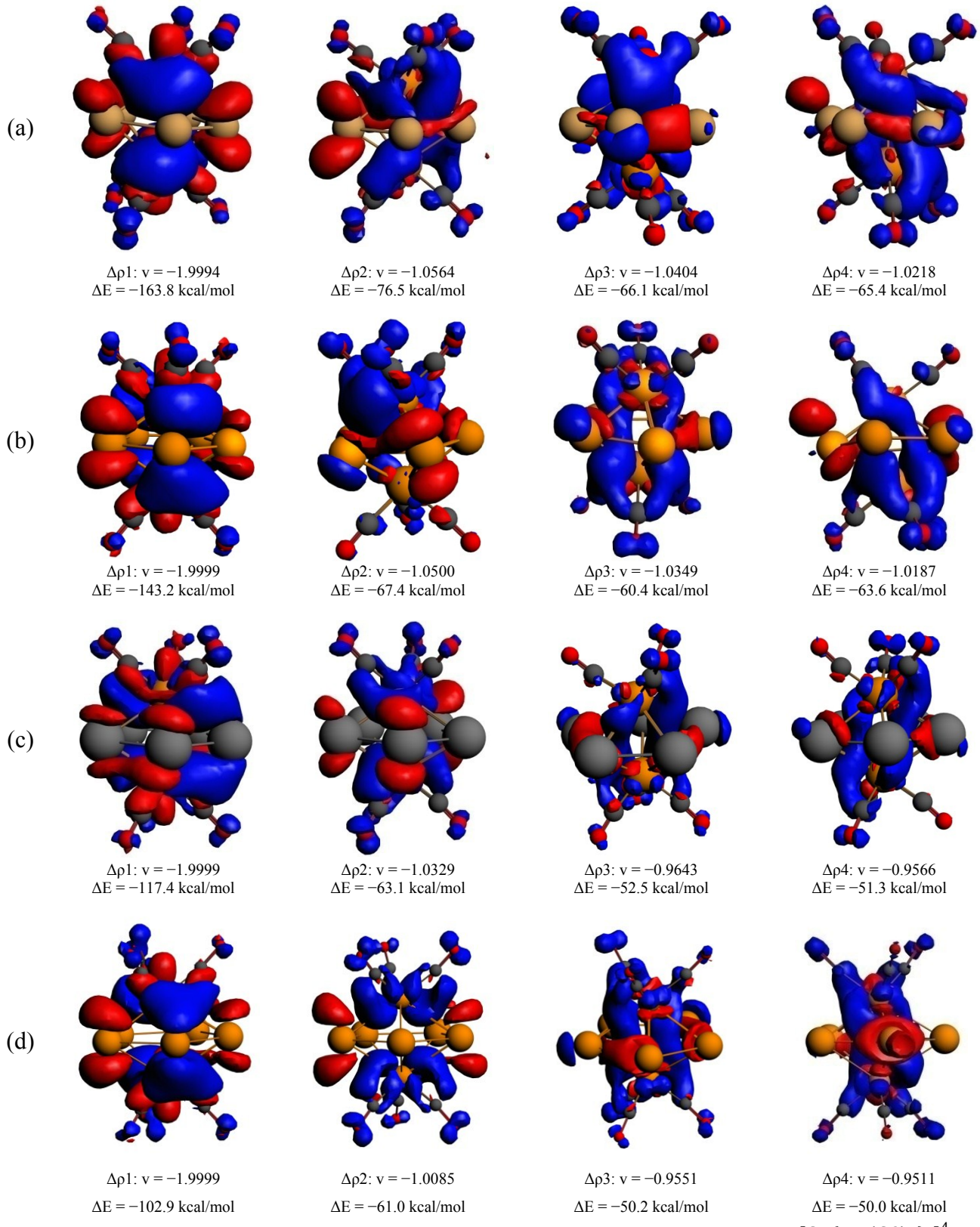

Figure S14. Deformation densities associated with the first four important orbital interactions for $[Si_5\{Mo(CO)_3\}_2]^{4-}$ (a), $[Ge_5\{Mo(CO)_3\}_2]^{4-}$ (b), $[Sn_5\{Mo(CO)_3\}_2]^{4-}$ (c) and $[Pb_5\{Mo(CO)_3\}_2]^{4-}$ (d) complexes, at BP86-D3/TZP(ZORA) level of theory.

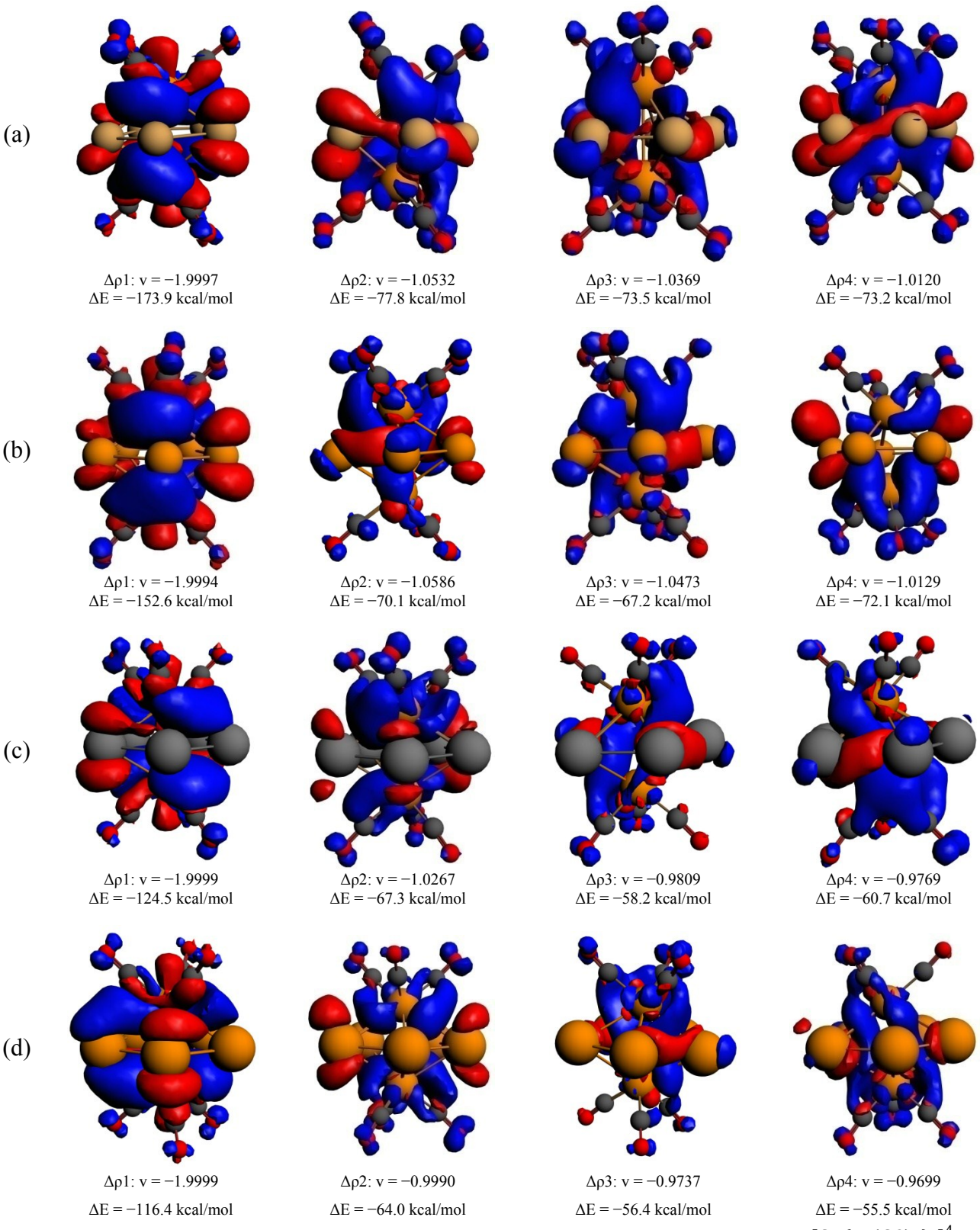

Figure S15. Deformation densities associated with the first four important orbital interactions for $[Si_5\{W(CO)_3\}_2]^{4-}$ (a), $[Ge_5\{W(CO)_3\}_2]^{4-}$ (b), $[Sn_5\{W(CO)_3\}_2]^{4-}$ (c) and $[Pb_5\{W(CO)_3\}_2]^{4-}$ (d) complexes, at BP86-D3/TZP(ZORA) level of theory.

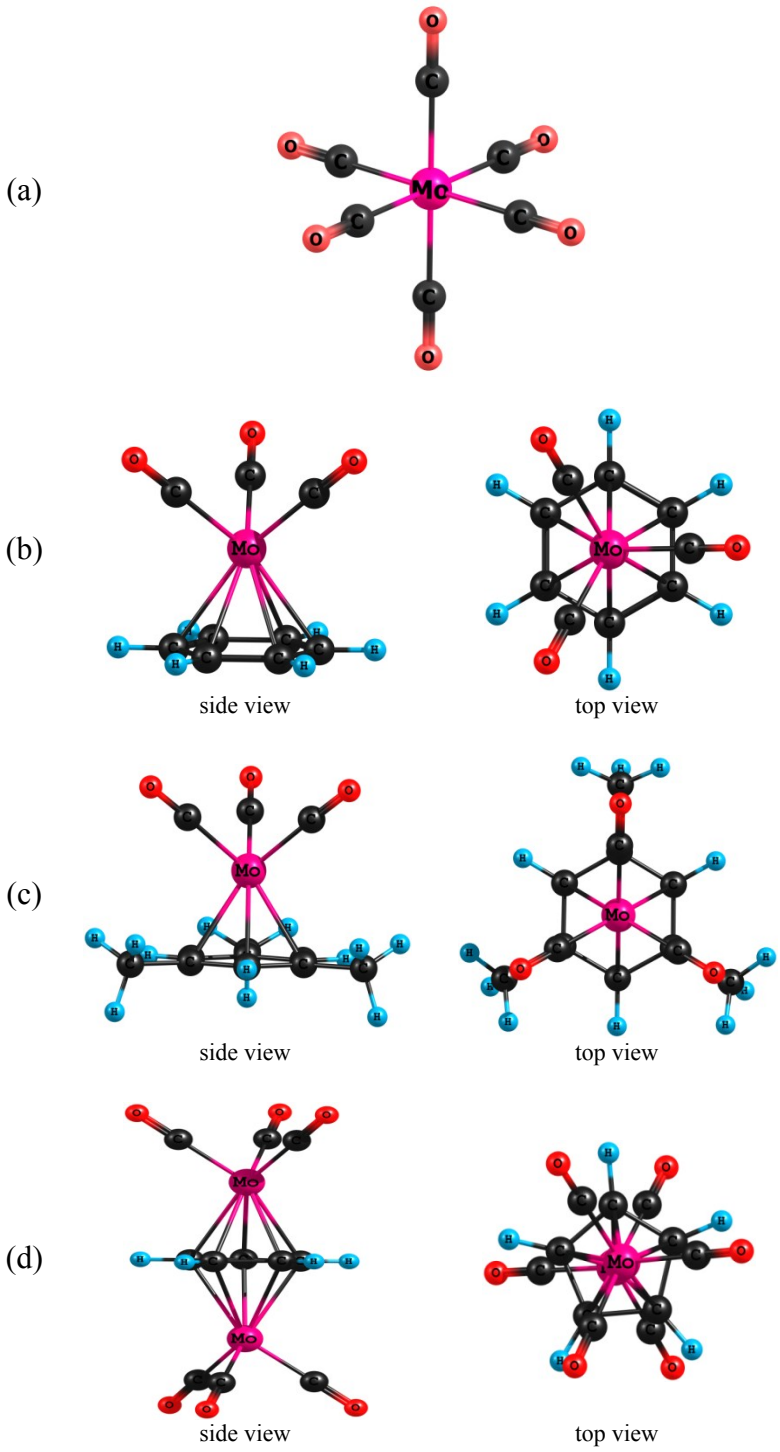

Figure S16. Optimized structures for $[Mo(CO)_6]$ (a), $[(\eta^6\text{-}C_6H_6)\{Mo(CO)_3\}]$ (b), $[Mes\{Mo(CO)_3\}]$ (c) and $[(\eta^5\text{-}C_5H_5)\{Mo(CO)_3\}_2]^-$ (d) complexes, at M06-2X/def2-TZVPP level of theory.